withdrawn

G 9/2

DYNAMIC FRACTURE ANALYSIS OF THERMAL SHOCK LOADING IN NUCLEAR PRESSURE VESSELS

P. C. GEHLEN, M. F. KANNINEN, G. T. HAHN

Battelle Columbus Laboratories, Applied Solid Mechanics Section, 505 King Avenue, Columbus, Ohio 43201, U.S.A.

C. H. POPELAR

Ohio State University, Columbus, Ohio 43214, U.S.A.

Summary

The propagation and eventual arrest of a preexisting flaw in a reactor vessel subjected to thermal shock is of prime importance in the analysis of nuclear reactor safety. Four thermal shock experiments have been performed at Oak Ridge National Laboratories on thick walled cylinders (outside diameter 0.5m, wall thickness 146mm). However, observations on the smaller vessels cannot be related to large reactor pressure vessels (5m OD, wall thickness 0.2m) unless an analysis is available to connect the two sets of conditions.

Although several fracture analyses are available, their critical evaluations have been confined mainly to run-arrest events in small laboratory test pieces. The two-dimensional, dynamic, linear elastic, finite difference code described in this paper is designed to analyze run-arrest events in thick-walled cylinders. Preliminary results obtained with this code were compared with observations obtained during the fourth ORNL thermal shock experiment (TSE-4) in which the open-ended cylinder was preheated to 291°C and then cooled by pumping a fluid at -25C through its interior cavity. In this experiment, designed to simulate conditions similar to those encountered by a PWR (pressurized water reactor) vessel during a hypothetical loss-of-coolant accident, the crack driving force is provided by an adverse temperature gradient across the cylinder's wall. Experimentally, it was observed that the originally 11mm deep, long axial crack started propagating 150 seconds after the beginning of fluid injection into the cylinder and arrested after having propagated in a single jump to a depth of 23mm.

Although the results of our initial analysis of this event were in reasonable agreement with the ORNL experimental observations (the model crack propagated 6mm compared to 12mm in the actual experiment), at the time these computations were performed, the fast fracture resistance of the vessel steel--a necessary input to the dynamic analysis--was not well known. Since this time, this curve has been characterized better. In this paper, results obtained with this updated fracture resistance curve are found to be in better agreement with the ORNL experimental results.

In view of the short crack jump distances associated with TSE-4, it is not surprising that in this particular case, dynamic effects play only a minor role in the interpretation of the run-arrest event. However, in a hypothetical case where the fracture toughness was arbitrarily lowered to the point where the static analysis would predict that the crack

propagates from 11 to 105mm, the dynamic analysis predicts that the crack penetrates the wall completely.

1. Introduction

Although several numerical analyses have been shown to reproduce experimental observations on run-arrest events to a high degree of accuracy [1-3], their usefullness is primarily restricted to small laboratory test specimens. The Battelle two-dimensional, dynamic, linear elastic finite difference codes have been generalized and can now be used to analyze fast fracture events in cylindrical reactor pressure vessels. The usefullness of such an analysis in the study of reactor safety is obvious because the size of full-scale reactor vessels makes actual testing on such vessels extremely complex and expensive. Four thermal shock experiments on smaller vessels have been conducted at Oak Ridge National Laboratories [4]. However, results obtained with the smaller vessels cannot be readily extended to the larger ones unless a dynamic analysis is available.

The first step in using such an analysis as a predictive tool is to verify its accuracy in a case where reliable experimental data are available. The fourth ORNL thermal shock experiment (TSE-4) is well documented and was used as a benchmark to establish the validity of our analysis.

In this experiment, an open-ended cylinder (530mm OD, 230mm ID, and 930mm long) was preheated to a temperature of 291C, then thermally shocked by injecting a mixture of 40 wt% methyl alcohol and 60 wt% water at -25C into the interior cavity of the cylinder. The resulting thermal gradient across the cylinder's wall induces high tensile stresses and an appreciable stress intensity factor (K_I), which coupled with a reduction in fracture toughness (K_{Ic}) resulting from the drop in temperature near the interior wall, causes the existing 11mm deep long axial crack to propagate. However, as the crack tip approaches the outer wall, the thermally induced stresses decrease, causing K_I to increase less rapidly. K_{Ic} on the other hand increases more rapidly as a result of the increasing temperature. In TSE-4, the combination of these two effects resulted in crack arrest after a crack jump of 12mm.

Our preliminary computations for TSE-4 yielded a crack jump distance of 6mm [5,6] which is in reasonable agreement with the experimental value quoted above. The only input required by our analysis--besides the standard elastic constants--is the dependence of the fast fracture toughness, K_{ID}, on crack speed and temperature. The experimental data available at the time our preliminary computations were performed is shown in Figure 1 in the form of the dependence of K_{Ic} on temperature. Since at that time it was believed that the fracture in the quenched-only A508 steel proceeded by the ductile mode, it was assumed that the dependence of the toughness on crack speed was similar to the one depicted in Figure 2a, that is to say that if the crack jump distance is small and fracture proceeds at slow speeds, the fracture toughness is for all practical purposes, independent of crack speed and may be approximated by K_{Ic}. Therefore, we felt justified in using the dotted straight line in Figure 1 as input for the dependence of the fracture toughness, both on temperature and crack speed. At this time, however, scanning electron microscopy on fracture surfaces [7] indicates that at the temperatures relevant to TSE-4, fracture does not always proceed in the ductile mode (see Figures 2b and c) and all available experimental results indicate that at 78 and 126°C the dependence of the toughness on crack speed is as shown in Figures 2b and c. Although for small crack jumps, the toughness can still be assumed to be independent of crack speed, this constant is no longer equal to K_{Ic}, but to a value that is somewhat lower, K_{Im} (the minimum in the K_{ID} versus velocity curve). Estimates of K_{Im} at 77°C and 126°C were deduced from pop-ins and are 77 and 134 $MPam^{1/2}$ respectively. In light of these observations, the dependence of the fracture toughness (at small crack speed) on temperature is more accurately represented by the solid straight line shown in Figure 1. (This relation is given by the following equation: $K_{ID} = 1.1633T - 12.57$ where K_{ID} is in $MPam^{1/2}$ and T in °C.)

After a short review of the 2-dimensional finite difference analysis, the remainder of this paper will describe the results obtained with this updated K_{ID} dependence. Finally, the relavance of dynamic effects in the description of run-arrest events in cylindrical vessels will be discussed.

2. The Dynamic Finite Difference Analysis

The version of the Battelle analysis used to study TSE-4 describes the dynamic propagation of a crack emanating from the inner surface and propagating toward the outer surface of a thick walled circular cylinder. A complete description is given in Reference 8. Finite difference theory is used to integrate the nodal equations of motion. Inelastic deformations except those permitted within the confines of linear elastic fracture mechanics in the vicinity of the crack tip are neglected. The length of the cylinder and the length of the crack in the axial direction are assumed to be much greater than the radius of the cylinder and therefore the behavior of the cylinder and the crack are adequately described by the dynamic equations of plane strain theory of elasticity. The crack driving force is assumed to be an adverse temperature gradient and/or an internal pressure (the latter being zero in the specific case of TSE-4).

As is the case with any numerical scheme, the test piece must be discretized. The nodal grid used here is shown schematically in Figure 3. The mass of the cells are lumped at the nodes. During the dynamic event, the crack tip may advance from edge to center to edge, etc of successive nodal cells. However, it is confined to the plane of symmetry indicated in Figure 3. It was shown [8] that within the finite difference representation, the dynamic strain energy release rate, G_I, is simply the change per unit crack advance of the strain energies of the cells containing the crack tip before and after its advance, thus making it possible to express G_I as a function of the displacements of only a few nodes immediately adjacent to the crack tip.

2.1 Initial Conditions

Before a dynamic event can be modeled, the nodal displacements corresponding to the prescribed load must be obtained. In the case where the crack driving force is a thermal gradient, no closed-form analytical solution for the initial nodal displacement is available, and they must be obtained numerically. In the present case, a first approximation to these displacements is obtained from the linear elastic solution for an uncracked hollow cylinder whose inside and outside walls are at predetermined temperatures. In the next step, the nodes are allowed to "relax" using their equations of motion. Excess energy is gradually removed using the "energy quench method" [9] until each node finds its equilibrium position. During this phase, the experimentally measured temperatures are assigned to each node, and the crack is allowed to open while the crack tip is held fixed in its assigned position.

2.2 Dynamic Analysis

Once the initial configuration is obtained as described above, the first nodal bond near the crack tip is broken at time $t = 0$. The equations of motion are then integrated while at the end of each time step the strain energy release rate, K_I, is computed and compared to K_{ID}, the dynamic fracture toughness. If K_I is equal to or larger than K_{ID}, the next bond is broken. Otherwise, this procedure is continued until after a predetermined length of time (usually of the order of 100 microseconds) the above condition can no longer be met. At that time, the crack is considered to have arrested.

3. Results

The computations described below were performed using the following materials properties: Young's modulus: 0.19305 $MNmm^{-2}$, Poisson's ratio: 0.3, bar wave speed: 5000 m/sec, coefficient of thermal expansion: 11.7×10^{-6} $°C^{-1}$. The temperature gradient across the cylinder's wall providing the crack driving force was measured at the time when crack propagation started (150 seconds after the beginning of the injection of cooling fluid) and is shown in Figure 4.

3.1 Initial Configuration

Using these equilibrium nodal positions, the static stress intensity at initiation can be computed. Using widely different grid spacings, we computed $K_I = 112.25$ $MPam^{1/2}$ for $\Delta r = 2.92$mm and $\Delta\phi = 25.71°$ (see Figure 3) and $K_I = 107.2$ $MPam^{1/2}$ for $\Delta r = 1.62$mm and $\Delta\phi = 6.43°$. These values compare well to the value of 114 $MPam^{1/2}$ obtained using a finite element technique [4] and to the experimentally observed value of 108 $MPam^{1/2}$ (see Figure 1). The agreement between computed and experimental values implies that the crack tip is not blunted, which is indeed found to be the case. The agreement between K_I-values obtained using the finite difference and finite element schemes is not quite as good for larger a/w ratios. This is due to the relatively poor approximation by our model of the local bending that occurs near the crack tip as the uncracked ligament becomes smaller. However, since in the analysis of TSE-4 the crack tip remains near the interior wall, this discrepancy does not affect our results. The computed static values of K_I as a function of a/w are shown in Figure 4.

3.2 Dynamic Analysis

Using the K_{ID} versus temperature dependence shown in Figures 1 and 4, and, assuming that K_{ID} is independent of crack speed, it was found that the crack tip originally positioned 11mm from the interior wall propagated a distance of 9mm (see Figure 4) in 120 microseconds. To insure that the crack had indeed arrested, the computation was continued for 420 microseconds after the last bond was broken. This time is ample for elastic waves emanating from the crack tip at onset to return there after bouncing off the interior or exterior walls or after traveling along a circumference in the vicinity of the crack tip.

This computed crack jump distance is in excellent agreement with the experimental value of 12 ± 2mm. The small discrepancy could arise from the uncertainty in K_{ID}, which may be in error by as much as ± 10%.

From Figure 4, it is also obvious that crack arrest occurs very near the point of intersection of the K_I and K_{ID} curves (a/w = 0.14) which is of course the arrest point predicted by the static theory. From this observation, it is concluded that dynamic effects play a minor role in this particular run-arrest event. This is also reflected by the small amount of strain energy that is converted into kinetic energy, i.e. about 0.06 joules while for a typical compact tension specimen, this quantity was found to be in excess of 150 joules. Similar conclusions were reached from previous computations on thick walled cylinders [5].

Although this observation is not surprising in the case of a short crack jump distance, it cannot be assumed that dynamic effects may be neglected under a different set of circumstances. To examine this possibility, another analysis was performed assuming that the toughness was independent of both temperature and velocity and that fracture toughness was arbitrarily lowered to $22 MPam^{1/2}$. Otherwise, the model was not changed. As can be seen in Figure 4 for this particular K_{ID}, the static theory predicts arrest to occur at a/w = 0.71, i.e. a penetration slightly less than the maximum permissible penetration recommended by the ASME Boiler and Pressure Vessel Code [10].

The static theory assumes that none of the excess strain energy which is converted into kinetic energy is available to drive the crack at the time of arrest: it is either dissipated by damping or else does not perturb the static solution near the crack tip [6]. The dynamic analysis on the other hand assumes that at least part of this kinetic energy is made available before arrest occurs. The important role played by this returned energy is clearly demonstrated in the present computation since the dynamic analysis predicts that the crack would not arrest. It is interesting to note that at the time when the last bond was broken, the kinetic energy was 2.2 joules, i.e. about 35 times larger than in the case of TSE-4.

4. Conclusions

The results of the Battelle dynamic analysis applied to TSE-4 are in excellent agreement with experimental observation. The small remaining discrepancy between computed and experimentally observed crack jump distances may be a result of the inaccuracy with which K_{Im} as a function of temperature is determined experimentally.

For short flaw lengths, the computed value of the static stress intensity, K_I, agrees with values obtained using finite element techniques. It differs by about 6% from the experimentally determined value of K_{Ic}. This is well within the error range on this quantity, indicating that the original flaw was sharp, an observation verified experimentally. As a result of inadequate modelling of local bending near the crack tip, the agreement between K_I values, computed using finite difference and finite element techniques, becomes worse as the flaw penetrates further into the wall.

The analytical model shows that in the case of TSE-4, dynamic effects are negligible. This is not surprising because dynamic effecrs at arrest vanish in the limit of infinitesimally small crack jumps. Although in this case the jump distance is finite, it is less than 10% of the remaining uncracked ligament. In the case of a hypothetical long jump, it was however, shown that dynamic effects can play an important role.

5. Acknowledgements

This work was supported by the U.S. Nuclear Regulatory Commission.

References

[1] GEHLEN, P. C., POPELAR, C. H., and KANNINEN, M. F., "Modeling of Dynamic Crack Propagation: I. Validation of One-Dimensional Analysis" to appear in Int. J. of Fracture Mechanics, 1979.

[2] POPELAR, C. H. and GEHLEN, P. C. "Modeling of Dynamic Crack Propagation, II. Validation

of Two-Dimensional Analysis" to appear in Int. J. of Fracture Mechanics, 1979.

[3] KOBAYASHI, T. and DALLY, J. W., "Photoelastic Evaluation of the Method of Measuring Crack Arrest Toughness With A Tapered-DCB Specimen" presented at ASME/CSME Pressure Vessel and Piping Conference, Montreal, June 25-29, 1978.

[4] CHEVERTON, R. D., ISKANDER, S. K., and BOLT, S. E., Applicability of LEFM to the Analysis of PWR Vessels Under LOCA-ECC Thermal Shock Conditions, NUREG/CR-0107, ORNL/NUREG-40, October 1978.

[5] CHEVERTON, R. D., GEHLEN, P. C., HAHN, G. T., and ISKANDER, S. K., ASTM Symposium on Crack Arrest Methodology and Applications, Philadelphia, Nov. 6-7, 1978 (to be published)

[6] HOAGLAND, R. G., GEHLEN, P. C., ROSENFIELD, A. R., and HAHN, G. T., ASME Publication 78 Mat-16 (1978)

[7] HAHN, G. T., et al, "Critical Experiments, Measurements and Analyses to Establish a Cr-ck Arrest Methodology for Nuclear Pressure Vessel Steels", Fourth Annual Progress Report to the U.S. Nuclear Regulatory Commission, NUREG/CR-0057 (1978).

[8] HAHN, G. T. et al, as above, Third Annual Progress Report to the U.S. Nuclear Regulatory Commission, NUREG/CR-0057 (1978)

[9] GEHLEN, P. C., ROSENFIELD, A. R., and HAHN, G. T., J. of Appl. Phys., 39, 5246 (1968).

[10] ASME Boiler and Pressure Vessel Code, Section XI, Article 5000.

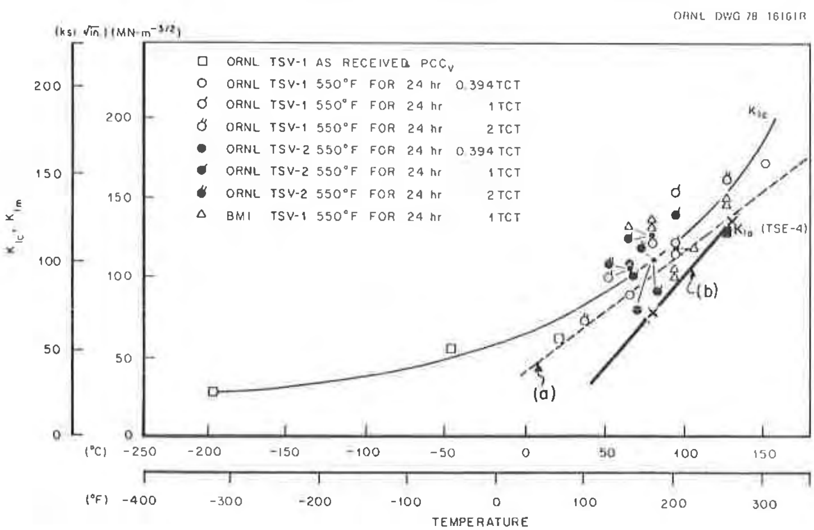

Figure 1. K_{Ic} versus temperature for quenched only A508 steel. Curve (a) represents the dependence of K_{ID} on temperature used in our preliminary computations (5,6) and curve (b) shows the relation used in this paper. The crosses (x) indicate experimental values for K_{Im}, the crack arrest toughness.

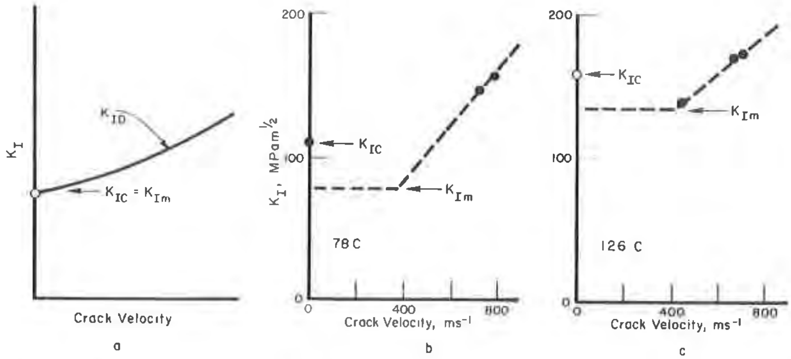

Figure 2. Dependence of fracture toughness on crack speed. (a) Schematic representation in the case where fracture proceeds in the ductile mode. (b) and (c) Quenched only A508 steel at 78C and 126C. The experimental points are indicated by o when fracture proceeds in the ductile mode and by • when fracture proceeds in the cleavage mode.

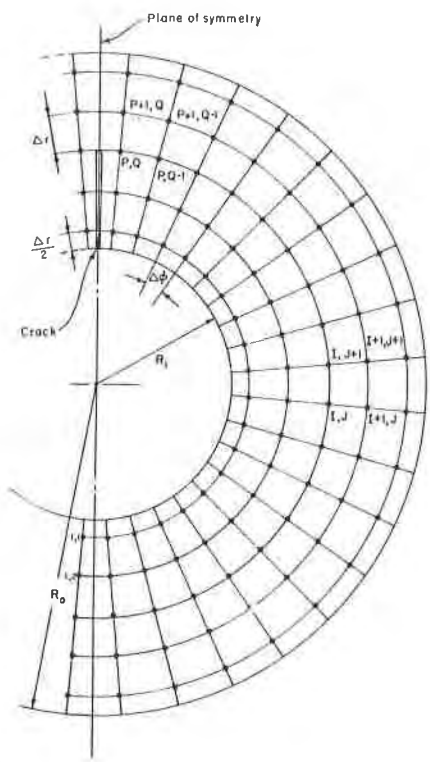

Figure 3. A finite difference net for a cracked thick walled cylinder.

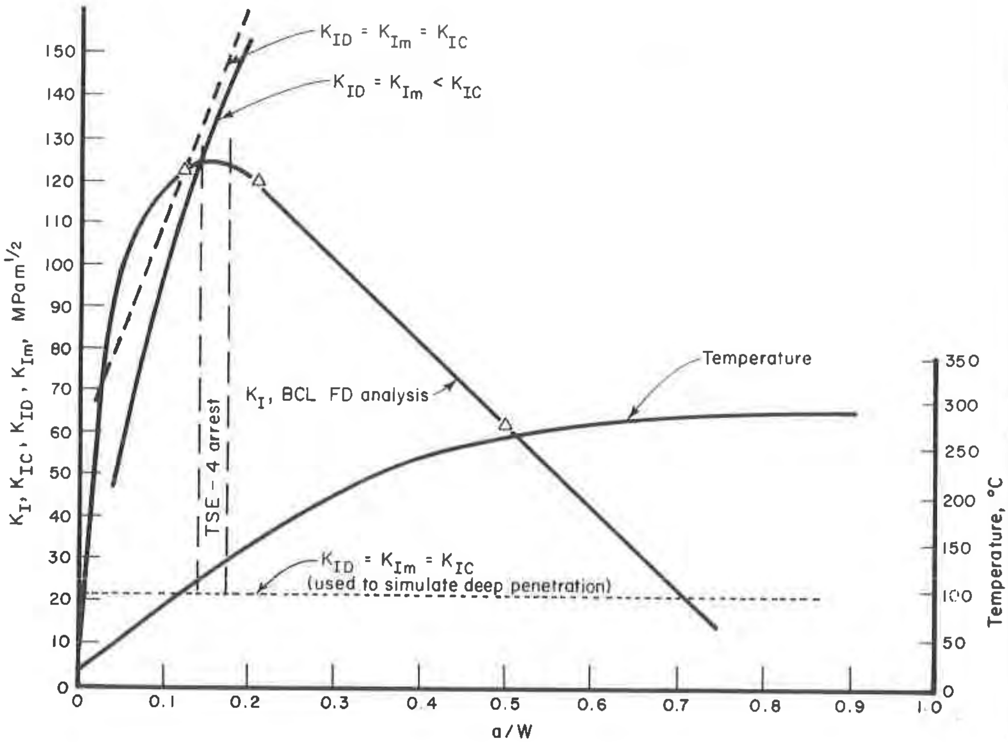

Figure 4. Analysis of run-arrest event in TSE-4.